Structure and low-temperature thermal conductivity of pyrolytic boron nitride

L. Duclaux,* B. Nysten, and J-P. Issi†
Unité de Physico-Chimie et de Physique des Matériaux, Université Catholique de Louvain, place Croix du Sud, 1, B-1348 Louvain-la-Neuve, Belgium

A. W. Moore
Union Carbide Coatings Service Corporation, 12900 Snow Road, Parma, Ohio 44130
(Received 11 February 1992)

The microstructure and morphology of three samples of pyrolytic boron nitride deposited at different temperatures have been characterized with use of x-ray diffraction and thermal-conductivity measurements. The x-ray analysis allowed the determination of the mean interlayer spacing, the out-of-plane coherence length, and the crystallites preferred orientation. It revealed the presence of three distinct morphologies. The thermal conductivity was measured as a function of temperature in the range $1.5 < T < 300$ K. The temperature variations of the thermal conductivity were fitted by using a model previously developed for the analysis of the thermal conductivity of graphites and carbons. This fit allowed the determination of the in-plane coherence length. It also allowed the analysis of point-defect concentration and of the interlayer shear modulus. It is shown that low-temperature thermal-conductivity measurements may be used to complement x-ray diffraction data for the microstructural characterization of materials.

I. INTRODUCTION

It has been previously shown how low-temperature thermal-conductivity measurements can be used as a tool for the microstructural characterization of layered materials such as graphites,[1] carbon fibers,[2,3] or pyrolytic boron nitride (PBN).[4] Particularly, this method allows the determination of the in- and out-of-plane coherence lengths.[2,3] While x-ray determination of crystallite sizes is limited to low values (approximately <100 nm), thermal-conductivity measurements present the advantage that they have no resolution limit. These measurements are thus a very useful complementary tool to x-ray diffraction for the microstructural characterization of materials. Advantages of thermal-conductivity measurements are also that extra information about the concentration of point defects and about mechanical parameters of the material may be obtained.[2,3]

Pyrolytic boron nitride presents a layered structure similar to that of graphite[5] except that the stacking of the layers is $AAA\ldots$ (Fig. 1). Along the c axis, a boron atom lies above a nitrogen atom alternatively. The in-plane distance between B and N atoms is 0.154 nm, and the interplanar distance c_0 is 0.333 nm. Sichel *et al.*[6,7] have also shown that boron nitride presents an anomalous difference between the temperature dependence of the lattice thermal conductivity ($\propto T^{2.4}$) and the specific heat which varies as T^3 below 10 K and at T^2 at higher temperatures. In fact, pyrolytic boron nitride presents a structure and a thermal conductivity behavior very similar to that of graphite.

Moore and Strong[8] have shown that pyrolytic boron nitride prepared at or near normal conditions can exhibit three distinct types of structure and morphology. The first is a turbostratic structure with an interlayer spacing d higher than 0.340 nm. The second is more crystalline ($d = 0.334$–0.335 nm). The third one presents an interlayer spacing similar to that of the second type, but consists of twinned columnar microcrystallites. Most samples contain more than one type of structure.

We have investigated samples of each structure and morphology prepared as described later. These samples were first characterized by specific-gravity measurements, x-ray diffraction, and x-ray fluorescence. More specifically, x-ray diffraction allowed the determination of the interplanar distance d, the c-axis stacking length L_c,

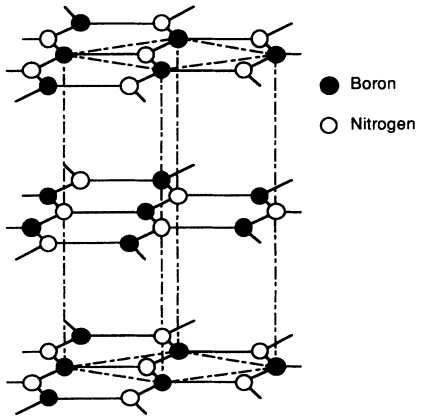

FIG. 1. Structure of crystalline hexagonal boron nitride. The layer stacking is $AAA\ldots$ with an interlayer spacing of 0.333 nm. The unit cell is represented by means of dot-dashed lines. The in-plane lattice constant a_0 is equal to 0.2504 nm, and the out-of-plane constant c_0 is equal to 0.6661 nm (Ref. 5).

and the crystallite orientation distribution $I(\Phi)$. For each sample, the structure and morphology of each were related to structural parameter values.[8]

We have measured the low-temperature thermal conductivity in the temperature range $1.5 < T < 300$ K. For the interpretation of the results, we have adapted the model developed for the thermal conductivity of graphite[2,3] to the case of hexagonal pyrolytic boron nitride. Using this model, we have fitted the experimental data and we obtained the following parameters: the a-axis crystallite size L_a, the interlayer shear modulus C_{44}, and quantitative information about point defects.

The paper is organized into four sections. In Sec. II the preparation and characterization methods are reported. In Sec. III the physical model used for the analysis of the thermal-conductivity results is explained. In Sec. IV the results of the structural characterization and thermal-conductivity measurements are presented. These results are discussed in Sec. V, and conclusions are given in Sec. VI.

II. EXPERIMENTAL DETAILS

The PBN samples investigated in this paper were prepared by reacting boron tricholoride and ammonia on hot graphite substrates in a pilot-plant-sized chemical-vapor-deposition (CVD) reactor at Union Carbide Coatings Service Corporation's laboratory in Parma, Ohio. Methods of x-ray characterization for the as-deposited PBN are given in Ref. 8.

The temperature variation of the thermal conductivity was measured in the temperature range $1.5 < T < 300$ K. The measurements were performed in a direction parallel to the deposition surface by means of a four-probe steady-state heat-flux method.[9] The samples dimensions were approximately $25 \times 10 \times 1$ mm^3.

The sample holder used for the measurements is presented in Fig. 2. The sample was thermally anchored at one end on a heat sink by means of low-temperature adhesive varnish (GE 7031) and secured by a copper plate and two screws. A heater consisting of a standard electronic metal-film resistor (1 kΩ) glued inside a copper block was fixed at the other end of the sample by means of adhesive varnish. The geometry of the heater was studied in order to have a good heat contact over the entire sample section.

According to the temperature investigated, the temperature gradient across the sample was measured either by means of two carbon-glass resistors [$(CG)_{hot}$ and $(CG)_{cold}$] previously calibrated ($T < 15$ K) or by means of two Chromel-Constantan thermocouples (T_{hot} and T_{cold}) ($T > 15$ K). The temperature sensors were mounted on copper plates attached to the sample by means of adhesive varnish. The temperature-sensor assemblies were supported by thin stainless-steel rods fixed by nuts on stainless-steel screws. The voltages of the temperature sensors were measured by means of a Keithley nanovoltmeter (K181), which has a resolution of 10^{-8} V.

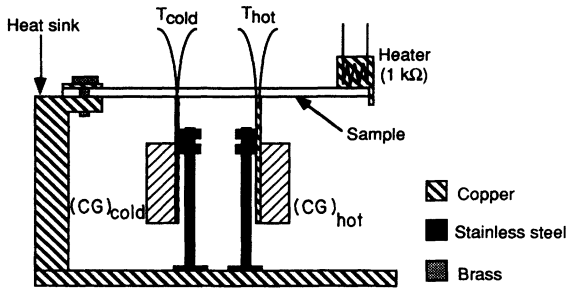

FIG. 2. Schematic representation of the experimental setup used for the thermal conductivity measurements (see text).

At 4.2 K the heat-loss conductance of the system was estimated to be of the order of 1 μW K^{-1}, which is more than an order of magnitude less than the conductances of the samples.

III. THEORETICAL MODEL

In electrically insulating materials, the thermal conduction is entirely due to quantified lattice vibrations, the phonons. The lattice thermal conductivity is limited by two distinct mechanisms: phonon-phonon scattering and phonon-defect scattering. At high temperatures, above the dielectric maximum, the thermal resistivity is due to phonon-phonon umklapp scattering. Around and below the dielectric maximum, the thermal conductivity is limited by the scattering of the phonons by static lattice defects. In the lowest-temperature range, boundary scattering is the dominating process. Near the dielectric maximum, scattering by small scale defects (i.e., points defects) may become the dominating process

In the relaxation time approximation, the lattice thermal-conductivity tensor components of a solid, $\kappa_{\alpha\beta}$, can be expressed by the relation[10]

$$\kappa_{\alpha\beta}=\frac{k_B}{8\pi^3}\sum_{p=1}^{3}\int_{BZ}\left[\frac{\hbar\omega_p(\mathbf{q})}{k_BT}\right]^2\tau_p(\mathbf{q})\{v_p(\mathbf{q})\}_a\{v_p(\mathbf{q})\}_b\frac{\exp[\hbar\omega_p(\mathbf{q})/k_BT]}{\{\exp[\hbar\omega_p(\mathbf{q})/k_BT]-1\}^{-2}}dq_xdq_ydq_z\ . \tag{1}$$

The summation is made over the three acoustic polarizations ($p=1$, 2, or 3), and the integration is made over the first Brillouin zone in reciprocal space. q_x, q_y, and q_z are the components of the wave vector $\mathbf{q}$ along the three directions in reciprocal space. $\omega_p(\mathbf{q})$ and $\tau_p(\mathbf{q})$ are, respectively, the frequency pulsation and relaxation time of a phonon with wave vector $\mathbf{q}$ and polarization p. $\{v_p(\mathbf{q})\}_\alpha$ is the group velocity in the α directions given by the derivation of $\omega_p(\mathbf{q})$ with respect to q_α.

As is the case for graphite, pyrolytic boron nitride presents a hexagonal symmetry which implies a reduction of the thermal-conductivity tensor to two components κ_a and κ_c. κ_a is the thermal conductivity parallel to the hexagonal layers (in-plane conductivity) and κ_c the thermal

conductivity perpendicular to the layers (out-of-plane thermal conductivity). If we suppose that the x and y axes lie parallel to the layers and the z axis parallel to the c axis, then $\kappa_a=\kappa_{xx}=\kappa_{yy}$ and $\kappa_c=\kappa_{zz}$.

The analogies between the structure and properties of graphite and hexagonal boron nitride enable us to apply the theory developed for the thermal conductivity of graphite to the case of boron nitride, as was previously done by Kelly[11] and Jager.[12]

First of all, the thermal conductivity has been measured along the deposition plane of samples that present crystallite misorientation with respect to this deposition surface. It implies that the measured thermal conductivity is a combination of the in-plane conductivity κ_a and the out-of-plane conductivity κ_c. Assuming that the deposition plane is $(x,y,0)$ and that the thermal conductivity is measured along the x axis, the measured thermal conductivity is then given by the relation[13]

$$\kappa_x=\kappa_z\left[1-\left[1-\frac{\kappa_c}{\kappa_a}\right]\langle\sin^2\phi\cos^2\psi\rangle\right], \tag{2}$$

with the mean value of $\sin^2\phi\cos^2\psi$ over all the samples given by

$$\langle\sin^2\phi\cos^2\psi\rangle=\frac{1}{2}\frac{\int_0^{\pi/2}I(\phi)\sin^3\phi\,d\phi}{\int_0^{\pi/2}I(\phi)\sin\phi\,d\phi}. \tag{3}$$

ϕ is the angle between the crystallite c axis and the z axis normal to the deposition plane. ψ is the angle between the x axis and the crystallite c-axis projection onto the deposition plane. $I(\phi)$ represents the crystallite orientation distribution function, which has been measured by x-ray diffraction.

Komatsu and Nagayima[14,15] developed a semicontinuum model for lattice dynamics in graphite valid at low temperature. This model gives the following dispersion relations for the three polarizations:

$$\omega_1(\mathbf{q})=\left[V_l^2q_a^2+4\frac{C_{44}}{\rho_m d^2}\sin^2\left[\frac{dq_c}{2}\right]\right]^{1/2}, \tag{4a}$$

$$\omega_2(\mathbf{q})=\left[V_t^2q_a^2+4\frac{C_{44}}{\rho_m d^2}\sin^2\left[\frac{dq_c}{2}\right]\right]^{1/2}, \tag{4b}$$

$$\omega_3(\mathbf{q})=\left[\delta^2q_a^4+\frac{C_{44}}{\rho_m}q_a^2+4\frac{C_{33}}{\rho_m d^2}\sin^2\left[\frac{dq_c}{2}\right]\right]^{1/2}. \tag{4c}$$

Polarizations 1 and 2 are, respectively, the two in-plane polarizations. Polarization 3 is the out-of-plane polarization. d is the interlayer spacing, q_a and q_c are, respectively, the wave-vector projections onto the layer planes and c axis, ρ_m is the mass density, δ is related to the bending modulus of the layers, C_{33} is the compression modulus, and C_{44} is the interlayer shear modulus. V_l and V_t are, respectively, the longitudinal and transverse in-plane phonon velocities related to the elastic moduli C_{11} and C_{12} by the relations

$$V_l=\left[\frac{C_{11}}{\rho_m}\right]^{1/2}, \tag{5a}$$

$$V_t=\left[\frac{C_{11}-C_{12}}{2\rho_m}\right]^{1/2}. \tag{5b}$$

In order to calculate the lattice thermal conductivity, we still have to define the phonon-scattering relaxation time. At low temperature, below the dielectric maximum, mainly two mechanisms, boundary scattering and point-defect scattering, lead to phonon scattering.[9]

So, for each polarization p, two relaxation times are considered: $\tau_{pB}(\mathbf{q})$, the relaxation time for boundary scattering, and $\tau_{pD}(\mathbf{q})$, the relaxation time for point-defect scattering. The total relaxation time is then given by

$$\frac{1}{\tau_p(\mathbf{q})}=\frac{1}{\tau_{pB}(\mathbf{q})}+\frac{1}{\tau_{pD}(\mathbf{q})}. \tag{6}$$

Concerning boundary scattering, as is the case for graphite, boron nitride crystallite may be represented by cylinders with diameters equal to L_a and height equal to L_c.[16] Phonons may be scattered by boundaries parallel to the planes or boundaries perpendicular to the planes. For instance, in a crystallite with L_a equal to L_c, a phonon whose velocity component along the a axis is greater than along the c axis is scattered by the boundary perpendicular to the planes.[2,3] In the opposite case, the phonon is scattered by the boundary parallel to the planes. The relaxation times for these two mechanisms are, respectively, given by the relations

$$\{\tau_{pB}(\mathbf{q})\}_a=\frac{L_a}{[v_p(\mathbf{q})]_a}, \tag{7a}$$

$$\{\tau_{pB}(\mathbf{q})\}_c=\frac{L_c}{[v_p(\mathbf{q})]_c}. \tag{7b}$$

In order to determine which phonons are scattered by each type of boundary, we have to express the equality between $\{\tau_{pB}(\mathbf{q})\}_a$ and $\{\tau_{pB}(\mathbf{q})\}_c$. This determines a surface in $\mathbf{q}$ space whose position is determined by the ratio L_a/L_c. Phonons whose wave vector remains inside the surface are scattered by the grain boundaries parallel to the planes, whereas phonons whose wave vector remains outside the surface are scattered by the grain boundaries perpendicular to the planes. Let us assume that the values of the L_a/L_c ratio encountered in pyrolytic boron nitride are nearly the same values as those found in pyrolytic graphite, i.e., from 2 for turbostratic materials to more than 10 in almost perfect materials.[17] Then we see that the scattering of the phonons by boundaries parallel to the layers is negligible for the two in-plane contributions to the thermal conductivity as a result of their large in-plane velocities. On the contrary, the out-of-plane thermal conductivity may be reduced by the scattering of phonons by the boundaries parallel to the layers.

Concerning point-defect scattering, we used the phonon mean-free-path relations developed by Kelly for graphite.[18] From these relations we derived the following expressions for the corresponding relaxation times:

$$\frac{1}{\tau_{1D}(\mathbf{q})}=\frac{A}{V_l^2}\omega_1^3(\mathbf{q}), \tag{8a}$$

$$\frac{1}{\tau_{2D}(\mathbf{q})}=\frac{A}{V_t^2}\omega_2^3(\mathbf{q})\ , \tag{8b}$$

$$\frac{1}{\tau_{3D}(\mathbf{q})}=\frac{1.8Ad}{\delta}\left[\frac{\rho_m}{C_{33}}\right]^{1/2}\omega_3^3(\mathbf{q})$$

$$\text{for } \omega_3<\frac{2}{d}\left[\frac{C_{33}}{\rho_m}\right]^{1/2}, \tag{8c}$$

$$\frac{1}{\tau_{3D}(\mathbf{q})}=\frac{3.6A}{\delta}\omega_3^2(\mathbf{q}) \quad \text{for } \omega_3>\frac{2}{d}\left[\frac{C_{33}}{\rho_m}\right]^{1/2}. \tag{8d}$$

In these relations A is a constant related to the defect concentration.

Using the relations developed here, it is possible to calculate the temperature variation of the thermal conductivity of pyrolytic boron nitride along the deposition plane below the dielectric maximum.

IV. RESULTS

The density and structural characteristics of the three as-deposited PBN samples are given in Table I. A deposition temperature of 1670 °C yielded low-density turbostratic PBN (BN Sample No. 1) with small crystallite size and an interlayer spacing 3% larger than that of ideal hexagonal BN. A high-density deposit (BN Sample No. 2) made at 2000 °C was more crystalline with an interlayer spacing only 0.5% larger than the ideal value. In spite of these differences, the preferred orientation, as defined by the full width at half maximum intensity of the (002) orientation distribution function ($\Delta\theta_{002}^{\mathrm{FWHM}}$) was the same for both samples. Attempts to dope PBN with zirconium while depositing at 1890 °C yielded a very-high-density material (BN Sample No. 3), which was somewhat more crystalline than BN Sample No. 2. The x-ray rocking curve for this unusual deposit, which contained no more than 1 ppm of zirconium, consisted of two peaks, each 8°–12° $\Delta\theta_{002}^{\mathrm{FWHM}}$ and separated by about 73°.

The temperature variation of the thermal conductivity of the three boron nitride samples is presented in Fig. 3. It is compared with the thermal conductivity of highly oriented pyrolytic boron nitride (HOPBN).[7]

As expected, the thermal conductivity increases when crystalline ordering increases. The turbostratic sample (BN Sample No. 1) presents thus the lowest thermal conductivity over the entire temperature range. At room temperature its thermal conductivity is equal to 30 $\mathrm{W\,m^{-1}K^{-1}}$. Compared with BN Sample No. 2, BN Sample No. 3, which was tentatively doped during fabrication, presents an enhanced thermal conductivity. At 300 K they present, respectively, thermal-conductivity values of 150 and 225 $\mathrm{W\,m^{-1}K^{-1}}$. All three samples present lower values of thermal conductivity than HOPBN (Refs. 7 and 19) with a dielectric maximum arising at higher temperatures.

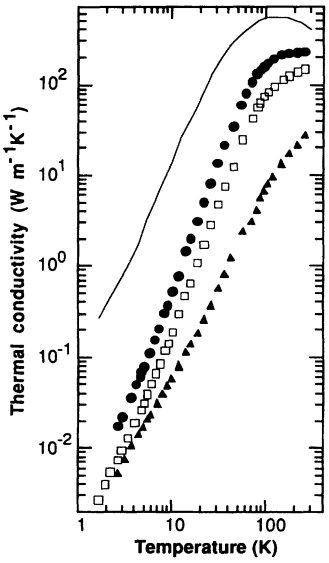

FIG. 3. Temperature variation of the thermal conductivity of the three pyrolytic boron nitride samples investigated [BN Sample No. 1 (▲), BN Sample No. 2 (□), and BN Sample No. 3 (●)] compared with the thermal conductivity of highly oriented pyrolytic boron nitride (Ref. 7) (solid line).

Below 70 K the temperature dependence of the thermal conductivity of BN Sample No. 1 is proportional to T^2. This behavior is characteristic of turbostratic materials.[2,3] In this kind of material, the weak coupling between layers implies weak interlayer moduli (C_{33} and C_{44}) and gives rise to a quasi-two-dimensional behavior [$\kappa(T)\propto T^2$].[2,3,16]

Below 10 K, BN Samples Nos. 2 and 3 present thermal-conductivity temperature dependences proportional to $T^{2.3}$ and $T^{2.5}$, respectively. These temperature

TABLE I. Characteristics of the three BN samples investigated: T_d, the deposition temperature; ρ_m, the mass density; d, the interlayer spacing; L_c, the out-of-plane coherence length; $\Delta\theta_{002}^{\mathrm{FWHM}}$, the full width at half maximum of the crystallite distribution function; and the type of structure (I, turbostratic structure; II, high-density structure with one crystallite preferred orientation; and III, very-high-density structure with twined crystallites) (Ref. 8).

Samples	T_d (°C)	ρ_m ($\mathrm{g\,cm^{-3}}$)	d (nm)	L_c (nm)	$\Delta\theta_{002}^{\mathrm{FWHM}}$ (deg)	Structure type
BN Sample No. 1	1670	1.80	0.343	6.0	65	I
BN Sample No. 2	2000	2.21	0.334–0.335	11.7	65	II
BN Sample No. 3	1890	2.23	0.334–0.335	13.3	82[a]	III

[a]Effective full width at half maximum across two peaks, each 8°–12° wide and separated by about 73°.

dependences are in agreement with those previously observed on HOPBN (Ref. 7) and on commercial BN[20], i.e., proportional to $T^{2.4}$. However, in the temperature range $10 < T < 70$ K, the temperature dependences are steeper ($\propto T^{2.8}$). We checked with a standard sample that this effect was not due to an experimental error. The same anomaly has also been observed by Jager.[12] Up to now, no satisfactory explanation can account for this behavior.

V. DISCUSSION

The temperature variation of the thermal conductivity below the dielectric maximum was fitted using the theoretical relations developed in Sec. III.

In the dispersion relations (4), we used the mass density ρ_m and the interplanar distance d given in Table I.

For the mechanical constants, we assumed that, as for the case of graphite, boron nitride intralayer moduli are not much affected by disorder.[2,3,21] So we assumed that the C_{11} and C_{12} values are constant for each sample. We used the values of C_{11} and C_{12} determined by Jager for pyrolytic boron nitride,[12] respectively, 750 and 150 GPa. These values of C_{11} and C_{12} are close to those determined by Kelly for HOPBN.[4] For δ, the constant related to the bending modulus, we used the value employed by Kelly[4] and Jager[12] (4×10^{-7} m^2 s^{-1}).

In graphites and carbons, C_{33} is supposed to be linearly related to interlayer distance d.[2,3,21] We made the same assumption for pyrolytic boron nitride. By an ultrasonic method, Jager has determined two experimental values of C_{33} for two pyrolytic boron nitride samples of different interlayer spacings.[12] These results provided us the following relation between compression modulus C_{33} and the interplanar distance d:

$$C_{33} = 18.7 - 672.8[d(\text{nm}) - 0.333] \text{ GPa} . \quad (9)$$

The interlayer shear modulus C_{44} is also related to the miscrostructure of the material, but the relation is not straightforward. Thus it was one of the adjustable parameters.

For boundary scattering we used in relation (7b) the values of L_c determined by x-ray diffraction (Table I). The in-plane crystallite size L_a in relation (7a) and the constant for point-defect scattering, A, in relations (8) were the two other adjustable parameters for the fit.

In relation (3) the crystallite orientation distribution function $I(\phi)$ was approximated by a Gaussian whose width at half maximum is equal to the full width at half maximum of the distribution functions determined by x-ray diffraction (Table I). The results of the fit are presented in Table II.

As expected, the in-plane crystallite size L_a increases from the turbostratic sample (BN Sample No. 1) to BN Sample No. 3 (Table II). This increase parallels that of the out-of-plane coherence length L_c determined by x-ray diffraction (Table I). This increase also parallels that of the thermal-conductivity values at room temperature. The same behavior has been already observed in carbon fibers.[2,3] This is in fact due to the high Debye temperature of these materials. As a consequence, the crystallite size becomes the main parameter that has to be improved to increase the thermal conductivity of these materials even at high temperatures.

TABLE II. Results of the parameter adjustments on the temperature variation of the thermal conductivity: L_a, in-plane crystallite size; A, constant for point-defect scattering; and C_{44}, interlayer shear modulus, compared with the room-temperature thermal conductivity κ_{300}.

Sample	κ_{300} (W m^{-1} K^{-1})	L_a (nm)	A (10^{-23} m^2)	C_{44} (GPa)
BN Sample No. 1	30	6.7	4.360	<0.01
BN Sample No. 2	150	55.6	<0.01	2.52
BN Sample No. 3	220	178.0	0.098	1.54

The result of the adjustment of the point-defect constant A confirms that the turbostratic sample (BN Sample No. 1) is the most defective sample. BN Sample No. 3 contains more point defects than BN Sample No. 2. However, very few chemical impurities were detected by x-ray fluorescence. Then we can suppose that these defects are mainly structural defects such as vacancies or interstitial atoms.

Shear-modulus values of pyrolytic boron nitride determined by low-temperature thermal-conductivity or specific-heat measurements are generally higher than the values obtained by ultrasonic measurements.[12] As is the case for graphite, it is assumed that determination of C_{44} by ultrasonic methods in pyrolytic boron nitride is affected by the presence of free basal dislocations. On the contrary, the shear modulus determined by specific-heat or thermal-conductivity measurements is considered as the intrinsic interlayer shear modulus.[12,22]

Results of the shear-modulus adjustment show that BN Sample No. 1 presents a very low value of shear modulus. This confirms the conclusion drawn from the T^2 temperature dependence, i.e., that layers are weakly coupled in turbostratic materials, leading to weak interlayer moduli and to a quasi-two-dimensional behavior of the thermal conductivity.

The difference observed between the C_{44} values of Samples Nos. 2 and 3 may be related to the difference observed in the point-defect concentrations. BN Sample No. 3 seems to contain more defects, and it is possible that the presence of more interstitial atoms reduces the interlayer shear modulus.

VI. CONCLUSIONS

X-ray-diffraction studies have s ɔwn that three types of structure and morphology can be found in PBN made at or near "normal" deposition conditions from mixtures of boron trichloride and ammonia.

Low-temperature thermal-conductivity measurements, in the range 1.5–300 K, enable us to further characterize these three different types of PBN. Adapting a theoretical model previously developed for graphites, we are able to determine the in-plane crystallite size L_a of our samples and to compare their point-defect concentrations and interlayer shear moduli C_{44}.

The thermal conductivity is found to increase from BN

Sample 1 to BN Sample No. 3. The values found for the in-plane crystallite size L_a show the same trends, confirming the increasing crystalline order from the turbostratic sample to the very-high-density sample. It also suggests that this parameter is the most important for the determination of the thermal-conductivity value even at high temperature.

The results of the adjustment of the point-defect constant A and shear modulus C_{44} confirm that the turbostratic sample (BN Sample No. 1) presents the most defective structure with weak interlayer bonding. The slight difference observed between the shear moduli of the two other samples may be attributed to the higher point-defect concentration found in BN Sample No. 3.

We have thus shown that, as is the case in graphites and carbon fibers, low-temperature thermal-conductivity measurements may be used to characterize the structure of pyrolytic boron nitride. Especially, they usefully complement x-ray diffraction for the determination of the crystallite size.

ACKNOWLEDGMENTS

This work is part of the program "Action de Recherche Concertée" sponsored by the Belgian State (Ministry of Scientific Policy). Centre de Recherche sur la Matière Divisée is Unité Associée du Centre National de la Recherche Scientifique.

*Present address: Centre de Recherche sur la Matière Divisée, Université d'Orléans, rue de la Férollerie, 1[B], F-45071 Orléans CEDEX 2, France.

†To whom all correspondence should be addressed.

[1]B. T. Kelly and K. E. Gilchrist, Carbon 7, 355 (1969).

[2]B. Nysten, J-P. Issi, R. Barton, Jr., D. R. Boyington, and J. G. Lavin, Phys. Rev. B **44**, 2142 (1991).

[3]B. Nysten, Ph.D. thesis, Université Catholique de Louvain, Louvain-la-Neuve, 1991 (in French).

[4]B. T. Kelly, J. Nucl. Mater. **68**, 9 (1977).

[5]R. S. Pease, Acta Crystallogr. **5**, 356 (1952).

[6]E. K. Sichel, R. E. Miller, M. S. Abrahams, and C. J. Buiocchi, Phys. Rev. B **13**, 4607 (1976).

[7]E. K. Sichel and R. E. Miller, in *Thermal Conductivity 14,* Proceedings of the 14th I. T. C. C., 1975, edited by P. G. Klemens and T. K. Chu (Plenum, New York, 1976), p. 11.

[8]A. W. Moore and S. L. Strong, Ceram. Eng. Sci. Proc. **10**, 846 (1989).

[9]R. Berman, *Thermal Conduction in Solids* (Oxford University Press, Oxford, 1976).

[10]P. Carruthers, Rev. Mod. Phys. **33**, 92 (1961).

[11]B. T. Kelly, Philos. Mag. **32**, 859 (1975).

[12]B. Jager, Ph.D. thesis, Université de Grenoble, Grenoble, 1977 (in French).

[13]G. E. Bacon, J. Appl. Chem. **6**, 477 (1956).

[14]K. Komatsu and T. Nagamiya, J. Phys. Soc. Jpn. **6**, 438 (1951).

[15]K. Komatsu, J. Phys. Soc. Jpn. **10**, 499 (1955).

[16]B. T. Kelly, Carbon **5**, 247 (1967); **6**, 71 (1968); **6**, 485 (1968).

[17]I. L. Spain, in *Chemistry and Physics of Carbon 13,* edited by P. L. Walker, Jr. and P. A. Thrower (Dekker, New York, 1981), p. 119.

[18]B. T. Kelly, in *Chemistry and Physics of Carbon 5,* edited by P. L. Walker, Jr. (Dekker, New York, 1969), p. 119.

[19]A. Simpson and A. D. Stuckes, J. Phys. C **4**, 1710 (1971).

[20]T-C. Hsieh and A. C. Anderson, Rev. Sci. Instrum. **52**, 1919 (1981).

[21]M. S. Dresselhaus, G. Dresselhaus, K. Sugihara, I. L. Spain, and H. A. Goldberg, *Graphite Fibers and Filaments* (Springer-Verlag, Berlin, 1988).

[22]E. J. Seldin and C. W. Nezbeda, J. Appl. Phys. **41**, 3389 (1970).

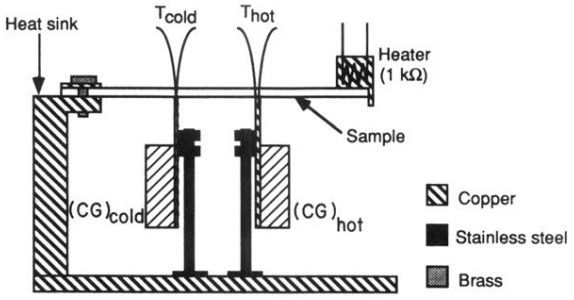

FIG. 2. Schematic representation of the experimental setup used for the thermal conductivity measurements (see text).